

Pozzolanic Reactivity and Hydration Products of Hedenbergite

Biyao Geng^{a,c,e,f}, Wen Ni^{b,c*}, Jiajia Wang^{b,c}, Xiajie Qiu^{b,c}, Xiaowei Cui^d, Chao Ren^{b,c}, Siqi Zhang^{b,c}, Yi Xing^a

^aSchool of Energy and Environment Engineering, University of Science and Technology Beijing, Beijing 100083, China

^bKey Laboratory of Ministry of Education of China for High-Efficient Mining and Safety of Metal Mines, School of Civil and Resources Engineering, University of Science and Technology Beijing, Beijing 100083, China

^cBeijing Key Laboratory on Resource-oriented Treatment of Industrial Pollutants, Beijing 100083, China

^dShangluo College, Chemistry and Chemical Engineering, Shangluo 726000, China

^eBeijing Weitong Environment Technology co., Ltd., Beijing 100144, China

^fBeijing Yujin Resources and Environment Technology Institute, Beijing 101502, China

niwen@ces.ustb.edu.cn

With hedenbergite, desulfurized gypsum and calcium hydroxide as the materials, this paper studies the pozzolanic reactivity of finely ground hedenbergite and performs XRD, IR, NMR and SEM analysis on the hydration products of the neat paste specimens. The results show that the compressive strength of the finely ground neat hedenbergite paste is 5.66MPa and 23.49MPa respectively at the age of 3d and 28d, which indicates that the finely ground hedenbergite has the pozzolanic reactivity, and that its hydration products are mainly C-S-H gel and ettringite. With the curing age, gypsum and silicate minerals are continuously consumed, the bonds connecting the silica tetrahedral network structures rupture, Si⁴⁺ is replaced by Al³⁺ disorderly, and the polymerization of the whole network is reduced, enhancing the activity and gradually increasing the hydration products.

1. Introduction

As of 2013, the comprehensive utilization of coal ash in the industrial solid waste had reached 69%, that of coal gangue 64%, and that of tailings only 18.9%. Most of the oxides in the tailings are similar to the raw materials required for cement production, which makes it possible to produce building materials using these tailings. Xuan et al., (2009) carried out an experimental study on sintering moderate heat portland cement with lead-zinc tailings. The results show that when lead-zinc tailings are used as ingredients, the mineral formation will be good and that the sinterability of clinker will be improved. Yousuf et al., (1993) performed FT-IR (Fourier Transform Infrared) test analysis and found that the tailings would produce a surface amorphous hydrate to prevent the hydration of C3S in the internal layer. Kutti et al., (1983) prepared a kind of cement-based material with ultra-high strength using mineral admixture. Other research results also indicate (Geng et al., 2015) that the silicate component and quartz in the tailings may be involved in the reaction that generates ettringite and C-S-H gel, so lead-zinc tailings can be used as active admixtures for concrete, and hedenbergite is a common mineral in lead-zinc tailings. In order to further understand the role of hedenbergite in the active admixture consisting of lead-zinc tailings, this paper prepares the neat paste specimen with hedenbergite as the main material and studies the pozzolanic reactivity and hydration products of hedenbergite, hoping to provide some basis for determining whether some tailings have pozzolanic reactivity.

2. Test materials and method

2.1 Test materials

(1) Hedenbergite: supplied by a company in Beijing. The chemical composition is shown in Table 1. It can be seen that, hedenbergite contains up to 49.86% of SiO_2 , and at the same time high content of MgO and CaO. Figure 1 is the XRD spectrum of hedenbergite.

(2) Natural gypsum: supplied by Beijing Fangshan Shuangshan Cement Plant. The chemical composition is shown in Table 1.

(3) Calcium hydroxide: produced by Sinopharm Chemical Reagent Co., Ltd., analytically pure.

Table 1: Main chemical components of hedenbergite (wt%)

Material	SiO_2	Al_2O_3	Fe_2O_3	FeO	MgO	CaO		
Hedenbergite	49.86	7.50	2.84	5.31	15.23	16.01		
Gypsum	3.91	3.61	0.19	0.33	8.94	30.93		
Material	Na_2O	K_2O	TiO_2	P_2O_5	MnO	Loss	S	
Hedenbergite	1.40	0.20	1.01	0.013	0.17	0.67	--	
Gypsum	0.15	0.25	0.080	0.017	0.081	25.49	26.28	

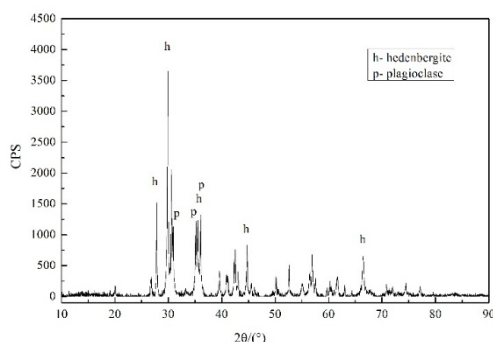


Figure 1: XRD spectrum of hedenbergite

2.2 Test method

First, use a jaw crusher to crush the hedenbergite, and then grind it in the sampling machine for 60min to obtain finely ground hedenbergite with a specific surface area of $624.3\text{m}^2/\text{kg}$.

Mix finely ground hedenbergite, natural gypsum and calcium hydroxide at a ratio of 91:3:6, and add 0.3% PC water reducer to prepare mixed dry powder (M). Then prepare a neat paste specimen with a size of $30\text{mm}\times 30\text{mm}\times 50\text{mm}$, with dry powder as the raw material and at a water-binder ratio of 0.20. Perform standard curing (at a temperature of $20\pm 1^\circ\text{C}$ and a humidity of no lower than 95%), and take samples respectively at the age of 3d, 7d and 28d, which are denoted as N1, N2 and N3. Perform XRD, SEM, IR and NMR. XRD analysis uses a Rigaku D/MAX-RC 12KW rotating anode diffractometer containing a Cu target, with a wave length of 1.5406\AA , an operating voltage of 40KV, an operating current of 150mA and a scanned range of $5^\circ < 2\theta < 90^\circ$. The SEM analysis uses an S250 scanning electron microscope, produced by Cambridge, with an acceleration voltage of 20kV. The IR analysis adopts an NEXUS70 fourier infrared spectrometer ($350\sim 7000\text{cm}^{-1}$), with a resolution of 3cm^{-1} . The working conditions are: humidity 68%, temperature 27°C , frequency 56~60Hz and voltage 220~240V.

3. Analysis and discussion

3.1 Compressive strength test on the neat hedenbergite paste specimen

Table 2 shows the test results of the compressive strength of the neat hedenbergite paste specimen at all ages.

As can be seen from Table 2, the compressive strength of the neat hedenbergite paste specimen increases from 5.66MPa at the age of 3d gradually to 23.49MPa at the age of 28d, indicating that the finely ground hedenbergite has pozzolanic reactivity.

Table 2: Compressive strength of the neat hedenbergite paste specimen at all ages

curing age	3d	7d	28d
compressive strength/ MPa	5.66	12.14	23.49

3.2 XRD analysis on the neat hedenbergite paste specimen

Figure 2 shows the XRD test results of the mixed dry powder and neat paste specimen of hedenbergite at all ages. As can be seen, the characteristic peak of calcium hydroxide ($2\theta \approx 18.04^\circ, 28.67^\circ, 34.04^\circ, 47.11^\circ, 50.81^\circ, 54.35^\circ, 62.63^\circ$ and 64.23°) is gradually weakened with the age^(Yang et al., 2000), until the age of 28d, when part of the peak almost disappears, indicating that at the age of 28d, the vast majority of calcium hydroxide has been consumed. The characteristic peak of gypsum ($2\theta \approx 11.63^\circ, 20.72^\circ$ and 29.11°) almost disappears at the age of 3d, indicating that, at this age, the gypsum has almost been consumed. The characteristic peak of ettringite ($2\theta \approx 9.16^\circ, 15.68^\circ, 23.03^\circ, 32.10^\circ$) appears at the age of 3d and gradually increases with the age, indicating that ettringite is generated in the reaction. Within the 2θ angle (26° - 34°) where typical C-S-H gel^(Yilmén et al., 2009) can easily cause protrusion in the XRD spectra (26° - 34°), in the XRD spectra of the samples in this experiment, with the curing age, the background value increases and small convex hulls appear, indicating that the C-S-H gel in the samples is on the growing trend with the curing age. The generation of ettringite and C-S-H gel is the reason why the strength of the neat paste specimen increases.

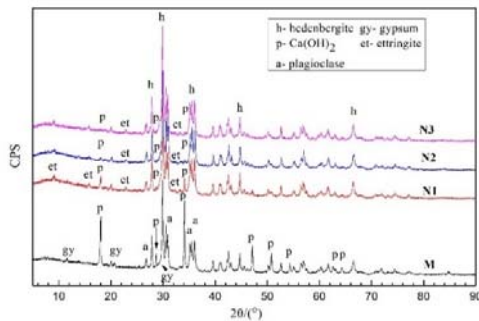


Figure 2: XRD spectra of mixed dry powder and neat paste specimen of hedenbergite at all ages (M: dry power, N1: 3d, N2: 7d, N3: 28d)

3.3 SEM analysis on the neat hedenbergite paste specimen

Figure 3 shows the SEM images of the neat hedenbergite paste specimen at all ages, of which (a), (b) and (c) are the images at the age of 3d, 7d and 28d respectively and (d) is the partial enlarged image of (c).

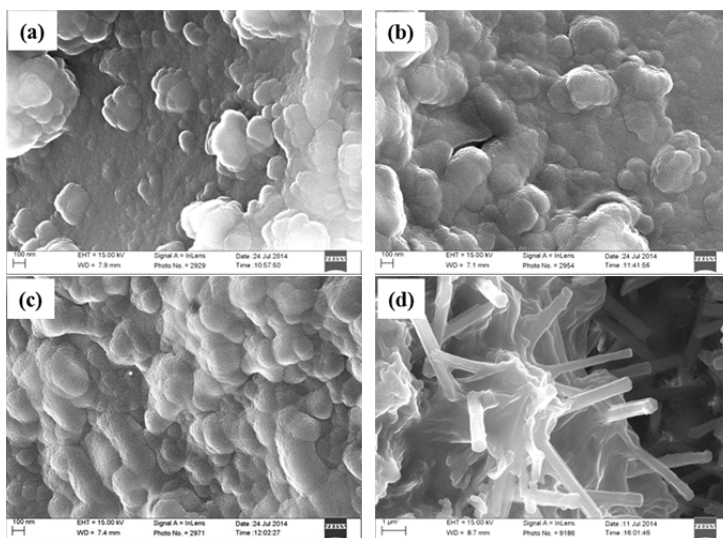


Figure 3: SEM images of neat hedenbergite paste specimen at all ages

It can be seen from Figure 3(a) that C-S-H gel has been formed in the 3d age system, and there are certain gaps between the finely ground hedenbergite particles. C-S-H gel contains some particles with a size of less than 100nm. Since the finely ground hedenbergite contains no particle smaller than 100 nm in size, it can be deduced that particles smaller than 100 nm may be C-S-H gel particles.

It can be seen from Figure 3(b) that the structure of the system at the age of 7d is denser than that at the age of 3d. The gaps between hedenbergite particles are narrowed, the connections between particles are stronger and the layering is more obvious.

It can be seen from Figure 3(c) that the system structure at the age of 28d is very compact. The finely ground hedenbergite particles have been covered by a large amount of C-S-H gel and the connections between the particles are tighter than at the age of 7d. The C-S-H gel particles have become very full and closely intertwined, looking like waves.

It can be seen from Figure 3(d) that there are a large amount of ettringite in the system, with the length of the needle- and rod-shaped ettringite being about $2\mu\text{m}$ and the diameter being about $0.35\mu\text{m}$, and they are connected together.

3.4 FT-IR analysis on the neat hedenbergite paste specimen

Figure 4 is the FT-IR spectra of the mixed dry powder and neat paste specimen of hedenbergite at all ages.

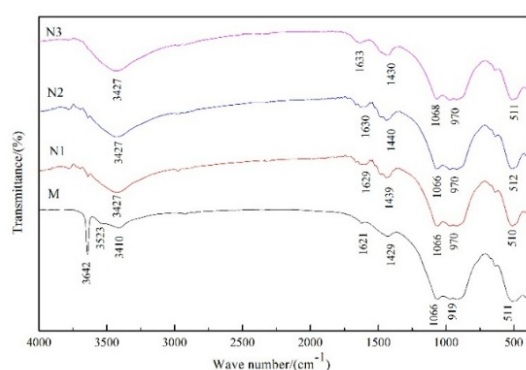


Figure 4: FT-IR spectra of mixed dry powder and neat paste specimen of hedenbergite at all ages (M: dry powder, N1: 3d, N2: 7d, N3: 28d)

The absorption peak at the range from 3800cm^{-1} to 3000cm^{-1} is the stretching band of the O-H bond of different substances in the system, and the absorption peak at 3642cm^{-1} is the asymmetric stretching vibration absorption center of the O-H bond in calcium hydroxide (Ylmén et al., 2009; Mollah et al., 2000). This absorption center is gradually weakened with the growth of the age and almost disappears at the age of 28d, indicating that with the hydration reaction going on, the vast majority of calcium hydroxide is consumed. The non-bulgy absorption peak near 3523cm^{-1} is the vibration peak of the O-H bond of the crystal water in gypsum (Ylmén et al., 2009; Peng et al., 1991). The absorption peak here almost completely disappears at the age of 3d, indicating that as the hydration reaction proceeds, gypsum is almost completely consumed at the age of 3d. In the FT-IR spectrum of the mixed dry powder sample, the absorption peak at 3410cm^{-1} is the asymmetric stretching vibration peak of the O-H bond that connects silica, and the surfaces of the fine particles of silicate minerals react with water molecules in the air to form such bonds. The surface of the finely ground hedenbergite is hydroxylated when in contact with the air, which also contributes to this peak at 3410cm^{-1} . In the FT-IR spectra of the samples, at the age of 3d, 7d and 28d, the absorption peak at 3427cm^{-1} is formed from the O-H bonds that connect silicon dioxide and the O-H bonds in ettringite and C-S-H gel. Note that from the mixed dry powder sample to those at the age of 3d, 7d and 28d, the wave number of the peak increases, indicating that the average bond energy of the O-H bonds increases with the age, and also shows that the average gravitational force that connects the O-H bonds and the cations is continuously weakened. The binding force between the bound water and cations in the newly generated ettringite and C-S-H gel is weaker than that between the bound water and the cations in the crystallized silicate minerals, so the bond energy of the O-H bond in the newly generated ettringite and C-S-H gel is higher than that of the O-H bond in silicate minerals. On the other hand, the continuous enhancement of the absorption band between 3800cm^{-1} and 3000cm^{-1} shows that the hydration reaction is ongoing with the age, which is consistent with the results obtained by XRD and SEM analysis.

The absorption peak at 1621cm^{-1} in the FT-IR spectrum of the mixed dry powder sample is the bending vibration peak of the O-H bond in the hydroxyl structural water or crystal water. In this system, the natural

gypsum in the mixed dry powder sample contributes to this peak. Similar absorption peaks also appear at 1629cm⁻¹, 1630cm⁻¹ and 1633cm⁻¹ at the age of 3d, 7d and 28d, respectively. It can be seen from the figure that both the wave number and sharpness of the absorption peak increase with the age, well indicating that gypsum is being constantly consumed and that the amounts of ettringite and C-S-H gel are increasing.

The absorption peak at 1429cm⁻¹ in the FT-IR spectrum of the mixed dry powder sample is the stretching vibration peak of CO₃²⁻ (Ylmén et al, 2009, Trezza et al., 2001), which, in this system, is caused by the carbonization reaction between the components of the mixed dry powder sample and CO₂ in the air. Similar absorption peaks also occur at 1439cm⁻¹, 1440cm⁻¹ and 1430cm⁻¹ at the age of 3d, 7d and 28d, respectively. The area of the absorption peaks is increasing, indicating that, during the preparation of the sample, the sample continues to react with CO₂ in the air and undergoes carbonation.

The absorption peaks near 511cm⁻¹ is the asymmetric bending vibration absorption peaks of the Si-O-Si bond in various complex silicate minerals and also the characteristic peaks of C-S-H gel (Lodeiro et al., 2009, Zhu, 1988). From the mixed dry powder sample to samples at the age of 3d, 7d and 28d, with the increase of age, the sharpness of the absorption peaks increases, indicating that the total amount of C-S-H gel in the system is increasing, while silicate minerals are being constantly consumed.

3.5 NMR analysis on the neat hedenbergite paste specimen

Figure 5 shows the ²⁹Si NMR spectra of the mixed dry powder and the neat paste specimen of hedenbergite at all ages. The XRD test results in Figure 1 show that there is plagioclase in the system, which has an interior structure of framework silicate with aluminum, that is, Q⁴(mAl). The interior structure of hedenbergite is chain silicate structure, that is, the Q² structure is dominant. The main absorption peak near the -92.57ppm in the ²⁹Si NMR spectrum of the hedenbergite dry powder sample are the combined result of Q² and Q⁴(mAl) (Yang et al., 2000).

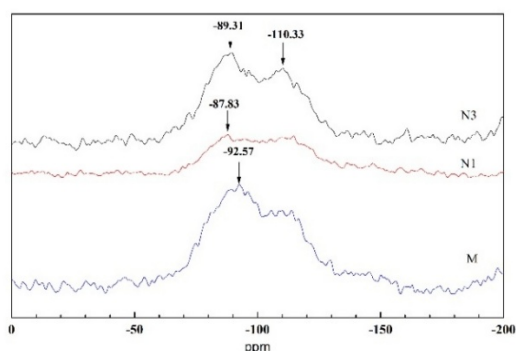


Figure 5: ²⁹Si NMR spectra of mixed dry powder and neat paste specimen of hedenbergite at all ages ²⁹Si (M: dry powder, N1: 3d, N3: 28d)

At the age of 3d, the height of the main peak at -92.57ppm is significantly reduced, and the width increases, and it shifts from -92.57ppm to -87.83ppm, showing a trend from high-field concentration to low-field dispersion. This is because during the early reaction stage, the silicon tetrahedron network in the system is excited by the chemical action of the hydroxide ions, and the bonds between network structures are broken, forming a single or silicon polyhedral structure with relatively low degree of polymerization. In addition, as there is Al³⁺ in the system, which is similar to Si⁴⁺ in size, Si⁴⁺ can be displaced by Al³⁺ disorderly, with the displacement quantity undetermined. At this point, the Al in tetrahedral coordination and Si together form the silicon aluminum oxide backbone, i.e. the Qⁿ(mAl) structure (m=1~4). The silicon-oxygen polyhedral network in the system is excited by the chemical action of hydroxide ions, making the bonds between network structures rupture, and at this time, the network intermediate Al in high coordination infiltrates, leading to the increase in the m value, making the chemical shift values of part of the strong peaks in the structure move towards the low field, so the polymerization degree of the entire network is reduced and the activity increases (He et al., 2007).

At the age of 28d, the main peak, whose height is originally greatly reduced at the age of 3d, rises again at -89.31ppm, and the peak position shifts towards the low field compared with that before the reaction, indicating that some of the structural forms that are more lowly-polymerized than the original system and with similar density of electron cloud around nucleus are getting more concentrated, which is consistent with the conclusion that the content of C-S-H gel increases with the reaction. From the age of 3d to 28d, the peaks at -110.33ppm are gradually getting more protruding. The peaks here are of the Q⁴ structure in the zeolite-like

phase, indicating that the zeolite-like phase within the system gradually increases as the reaction progresses. This also proves that there is plagioclase in the system, that is, $Q^4(mAl)$.

4. Conclusions

(1) With hedenbergite as the main material, this paper prepares the neat paste specimen, whose compressive strength is 5.66MPa and 23.49MPa respectively at the age of 3d and 28d, indicating that the finely ground hedenbergite has pozzolanic reactivity.

(2) According to the microanalysis results, the hydration products of hedenbergite are mainly C-S-H gel and ettringite. With the curing age, gypsum and silicate minerals are continuously consumed, the bonds connecting the silica tetrahedral network structures rupture, Si^{4+} is replaced by Al^{3+} disorderly, and the polymerization of the whole network is reduced, enhancing the activity and gradually increasing the hydration products.

Acknowledgments

The authors would like to thank the support from the National Key R&D Program of China (2017YFC0210301).

Reference

- Geng B.Y., Ni W., Wang J.J., Qiu X.J., Huang X.Y., 2015, An Initiative Investigation of the Pozzolanic Reaction of Ground Lead-Zinc Ore Tailings, *International Journal of Earth Sciences and Engineering*, 8, 1271-1278.
- He Y.J., Hu S.G., 2007, Application of ^{29}Si Nuclear Magnetic Resonance (NMR) in Research of Cement Chemistry, *Journal of Materials Science and Engineering*, 25, 147-153.
- Kutti, T., Malinowski, R., Srebnik, M., 1983, Investigation of mechanical properties and structure of alkaline activated blast-furnace slag mortars, *Silicon Industry*, 9, 175.
- Lee T.C., Wang W.J., Shih P.Y., 2009, Enhancement in early strengths of slag-cement mortars by adjusting basicity of the slag prepared from fly-ash of MSWI, *Cement and Concrete Research*, 39, 651-658.
- Lodeiro I.G., Macphée D.E., Palomo A, Fernández-Jiménez A, 2009, Effect of alkalis on fresh C-S-H gels. FTIR analysis, *Cement and Concrete Research*, 39, 147-153.
- Mollah M.Y.A., Yu W.H., Schennach R., Cocke D.L., 2000, A Fourier transform infrared spectroscopic investigation of the early hydration of Portland cement and the influence of sodium lignosulfonate, *Cement and Concrete Research*, 30, 267-273.
- Peng W.S., Liu G.K., 1991, Infrared spectra of gypsum and its thermal transformation products, *Acta Mineralogica Sinica*, 11, 27-32.
- Silva D.A., Roman H.R., Gleize P.J.P., 2002, Evidences of chemical interaction between EVA and hydrating Portland cement, *Cement and Concrete Research*, 32, 1383-1390.
- Trezza M.A., Lavat, A.E., 2001, Analysis of the system $3CaO \cdot Al_2O_3 - CaSO_4 \cdot 2H_2O - CaCO_3 - H_2O$ by FT-IR spectroscopy, *Cement and Concrete Research*, 31, 869-872.
- Xuan Q.Q., Li D.X., Luo Z.M., 2009, Lead-Zinc tailings applied in the production of moderate heat portland cement, *Journal of Materials Science and Engineering*, 27, 266-270.
- Yang N.R., Yue W.H., 2000, Atlas manual of inorganic non-metallic materials, Wuhan, Wuhan university of technology press.
- Ylmén R, Jäglid U, Steenari B.M., Panas I, 2009, Early hydration and setting of Portland cement monitored by IR, SEM and Vicat techniques, *Cement and Concrete Research*, 39, 433-439.
- Yousuf M., Mollah, A.S., Hess T.R., Tsai Y.N., Cocke D.L., 1993, An FTIR and XPS investigation of the effects of carbonation on the solidification/stabilization of cement based system-Portland Type V with zinc, *Cement and Concrete Research*, 23, 773-784.
- Zhu Z.X., 1988, Infrared spectrum research on garnets and clinopyroxenes in skarn lead-zinc, *Journal of Changchun University of Earth Science*, 4, 410-414.